
Figures and figure supplements

PTRN-1, a microtubule minus end-binding CAMSAP homolog, promotes microtubule function in *Caenorhabditis elegans* neurons

Claire E Richardson, et al.

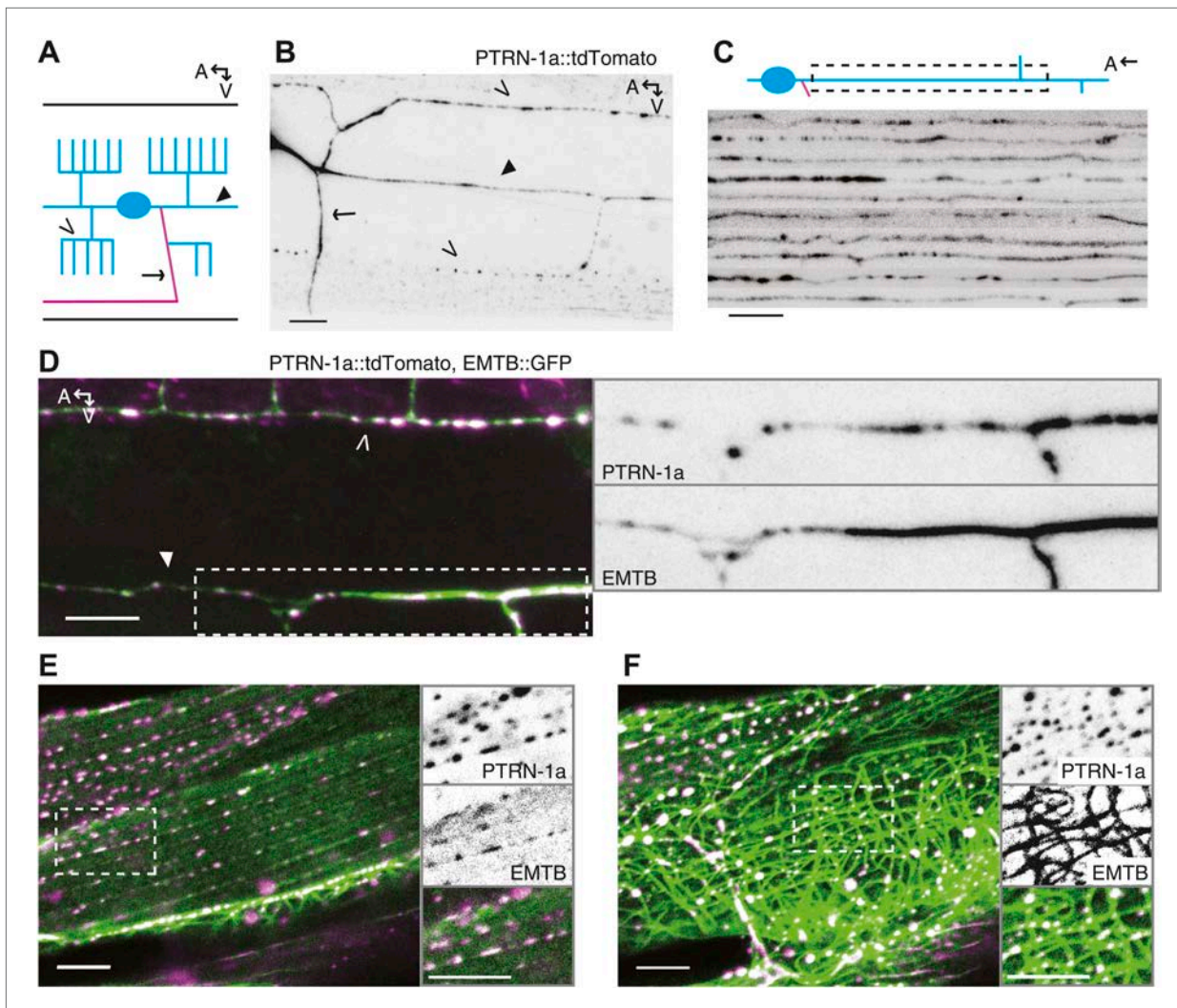


Figure 1. PTRN-1 localizes to puncta throughout neurites and colocalizes with MTs. **(A)** Schematic diagram of the central region of the PVD neuron. The cell body (blue oval) is in the posterior half of the animal. An elaborate dendritic arbor (blue lines) extends from the base of the head to the posterior of the animal, and the single axon (magenta) is extended into the ventral nerve chord (VNC). Black lines represent the outline of the animal. **(B)** PTRN-1a::tdTomato localization in the PVD neuron. The cell body is outside of the image, close to the left edge. **(C)** Confocal micrographs from 10 animals showing PTRN-1a::tdTomato localization in the PVD primary dendrite directly posterior to the cell body. **(D–F)** Colocalization of PTRN-1a::tdTomato (magenta) and EMTB::GFP (green) in the PVD neurites **(D)**, at the sarcolemma of the body wall muscle cells **(E)**, and in the cell interior of the body wall muscle cells **(F)**. Data were acquired from *wyEx5968* and *wyEx6022* transgenes coexpressed in the *ptrn-1(tm5597)* mutant. Closed arrowhead indicates the primary dendrite, the open arrowheads indicate tertiary dendrite, and arrow points to axon of the PVD neuron **(A, B, D)**. A, anterior; V, ventral. Scale bar: 5 μ m.

DOI: [10.7554/eLife.01498.003](https://doi.org/10.7554/eLife.01498.003)

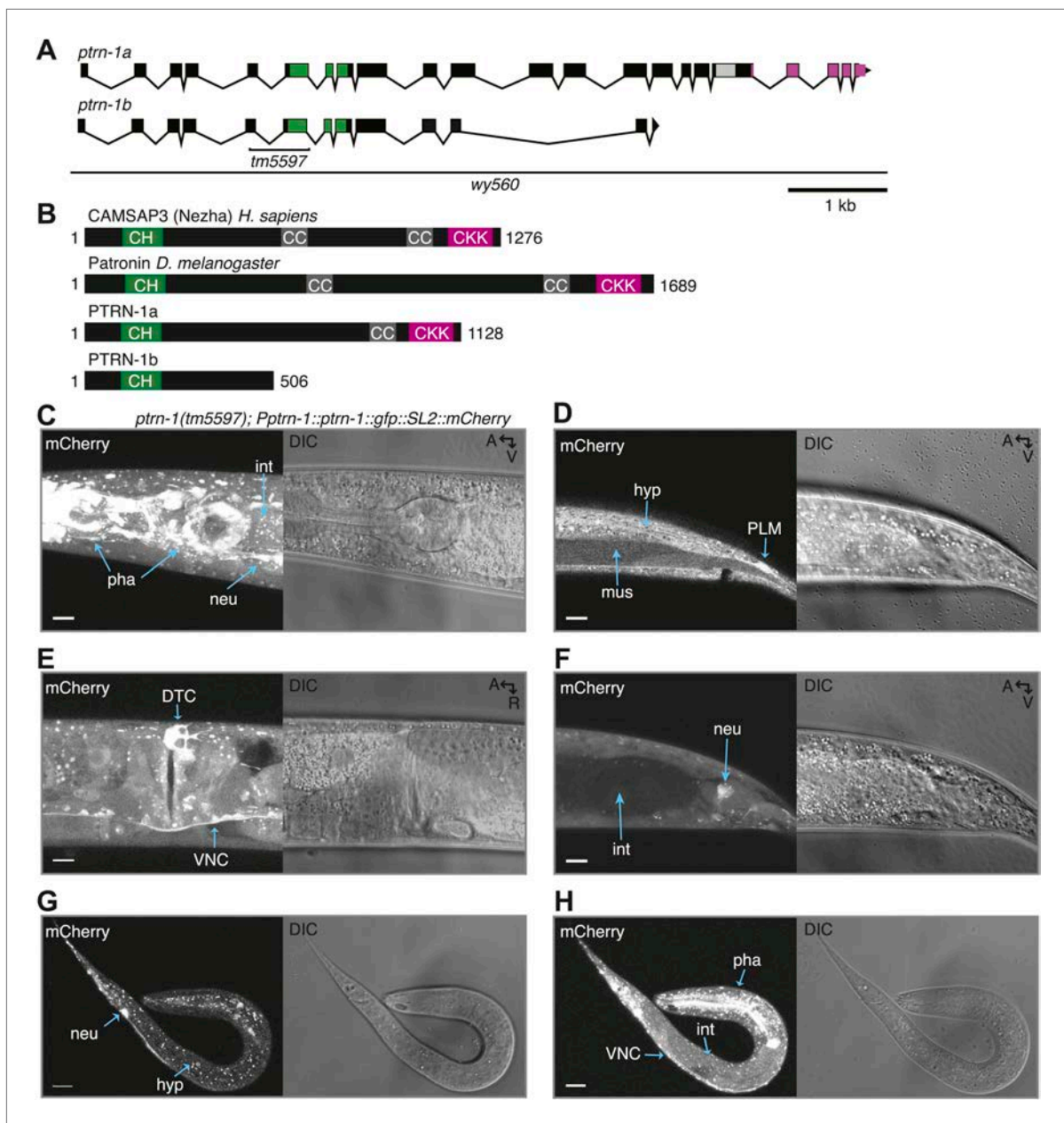


Figure 1—figure supplement 1. PTRN-1 is broadly expressed.

DOI: [10.7554/eLife.01498.004](https://doi.org/10.7554/eLife.01498.004)

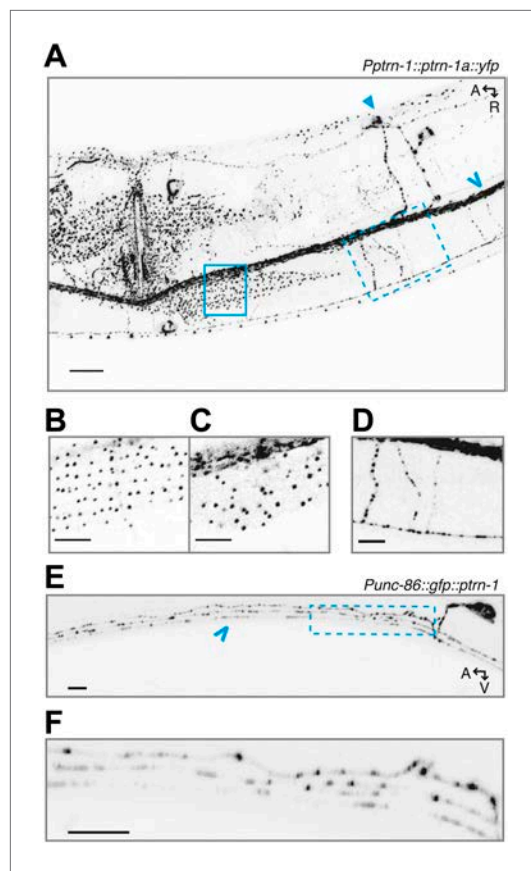


Figure 1—figure supplement 2. PTRN-1 exhibits punctate localization in neuronal processes and the body wall muscle cells.

DOI: [10.7554/eLife.01498.005](https://doi.org/10.7554/eLife.01498.005)

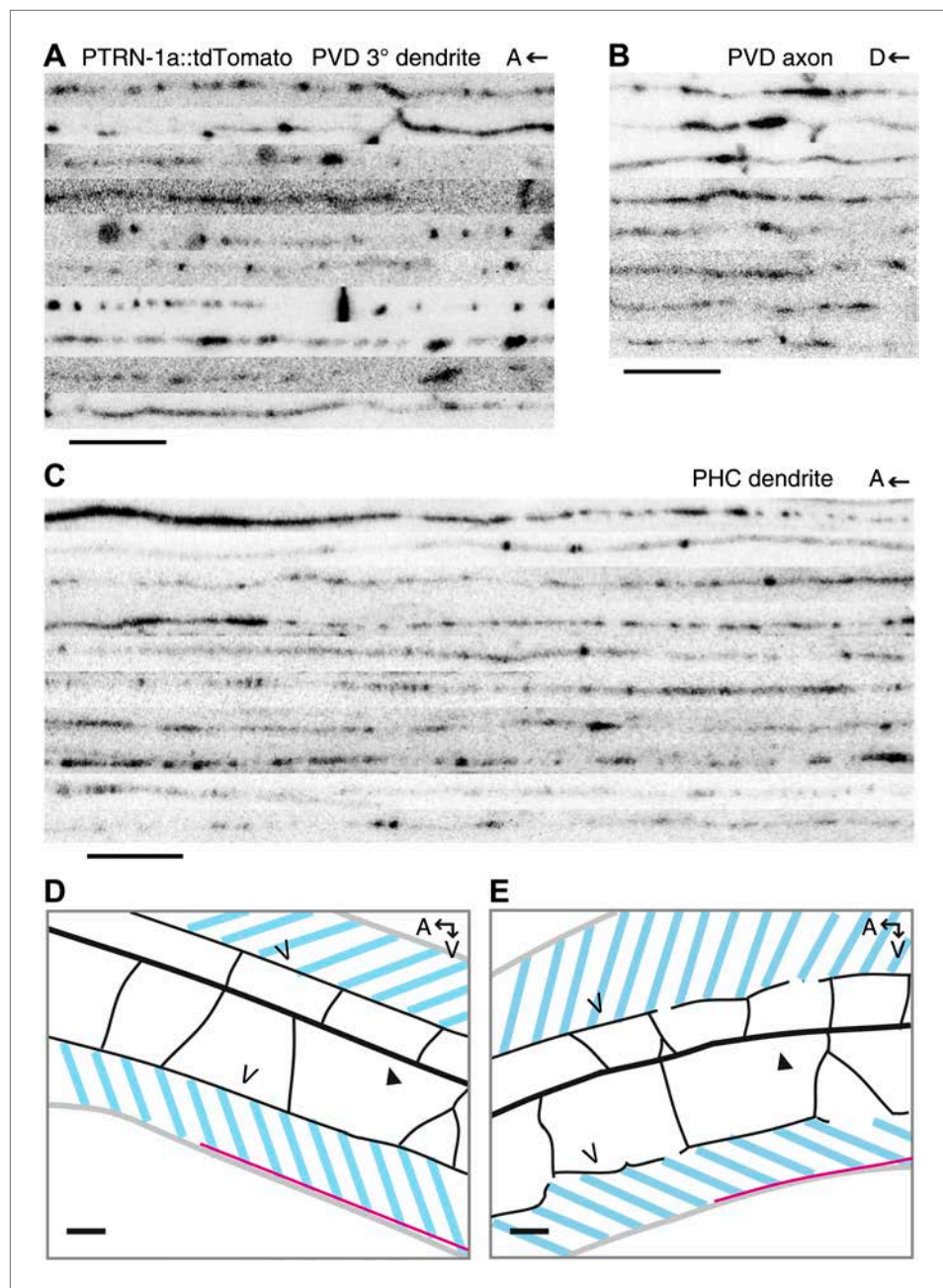


Figure 1—figure supplement 3. PTRN-1 localizes to puncta throughout the neurites in the PVD and PHC neurons.
 DOI: [10.7554/eLife.01498.006](https://doi.org/10.7554/eLife.01498.006)

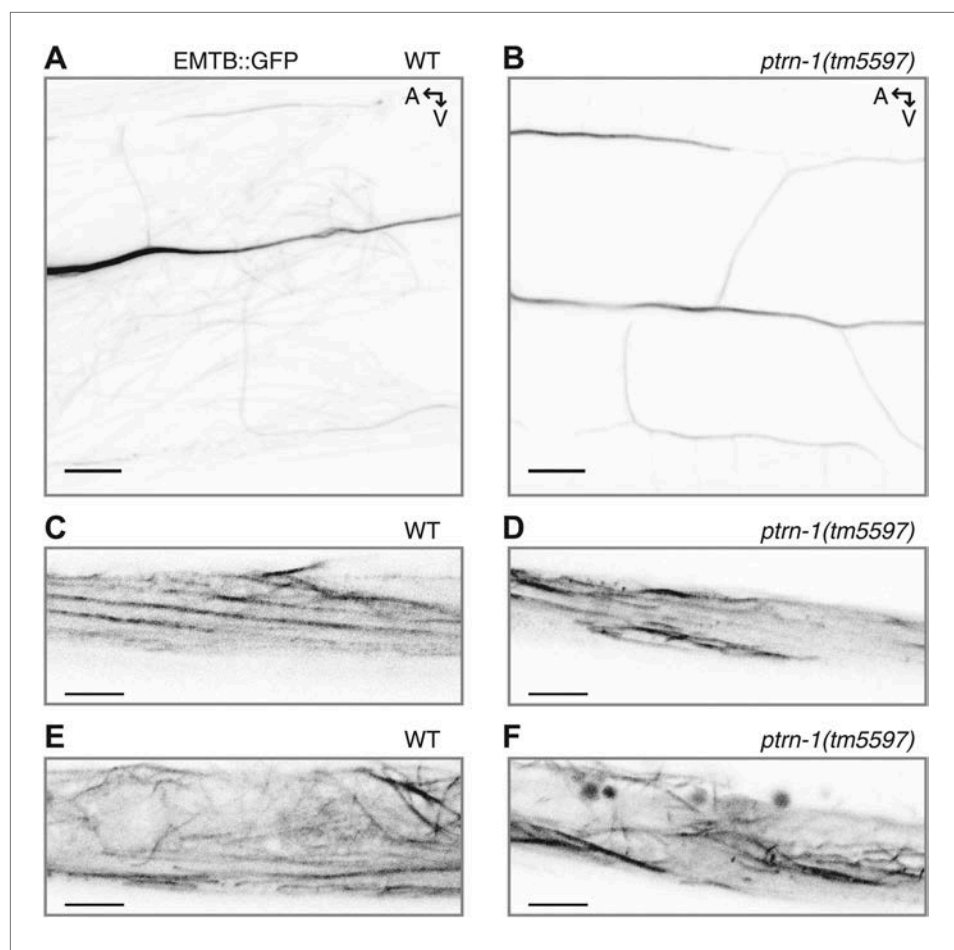


Figure 1—figure supplement 4. EMTB::GFP binds MTs in the PVD neuron and the body wall muscles.
DOI: [10.7554/eLife.01498.007](https://doi.org/10.7554/eLife.01498.007)

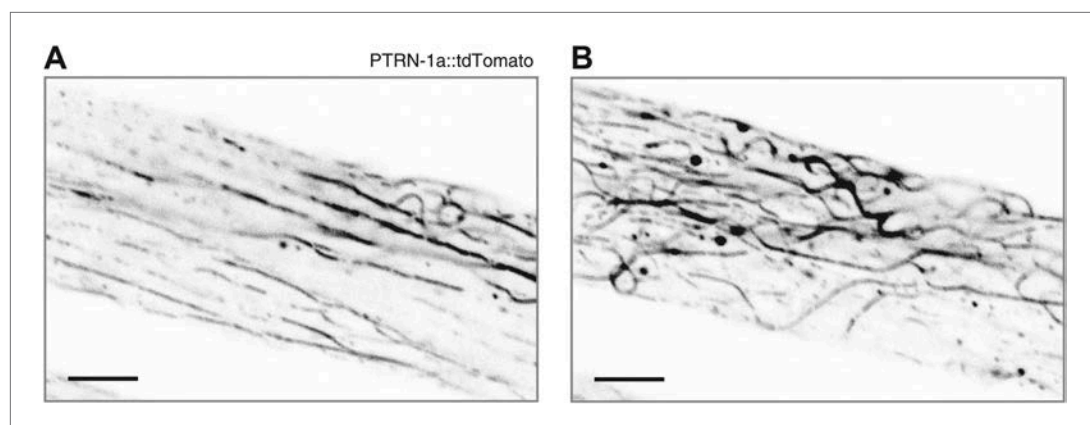


Figure 1—figure supplement 5. Highly expressed PTRN-1a::tdTomato binds along MT filaments.
DOI: [10.7554/eLife.01498.008](https://doi.org/10.7554/eLife.01498.008)

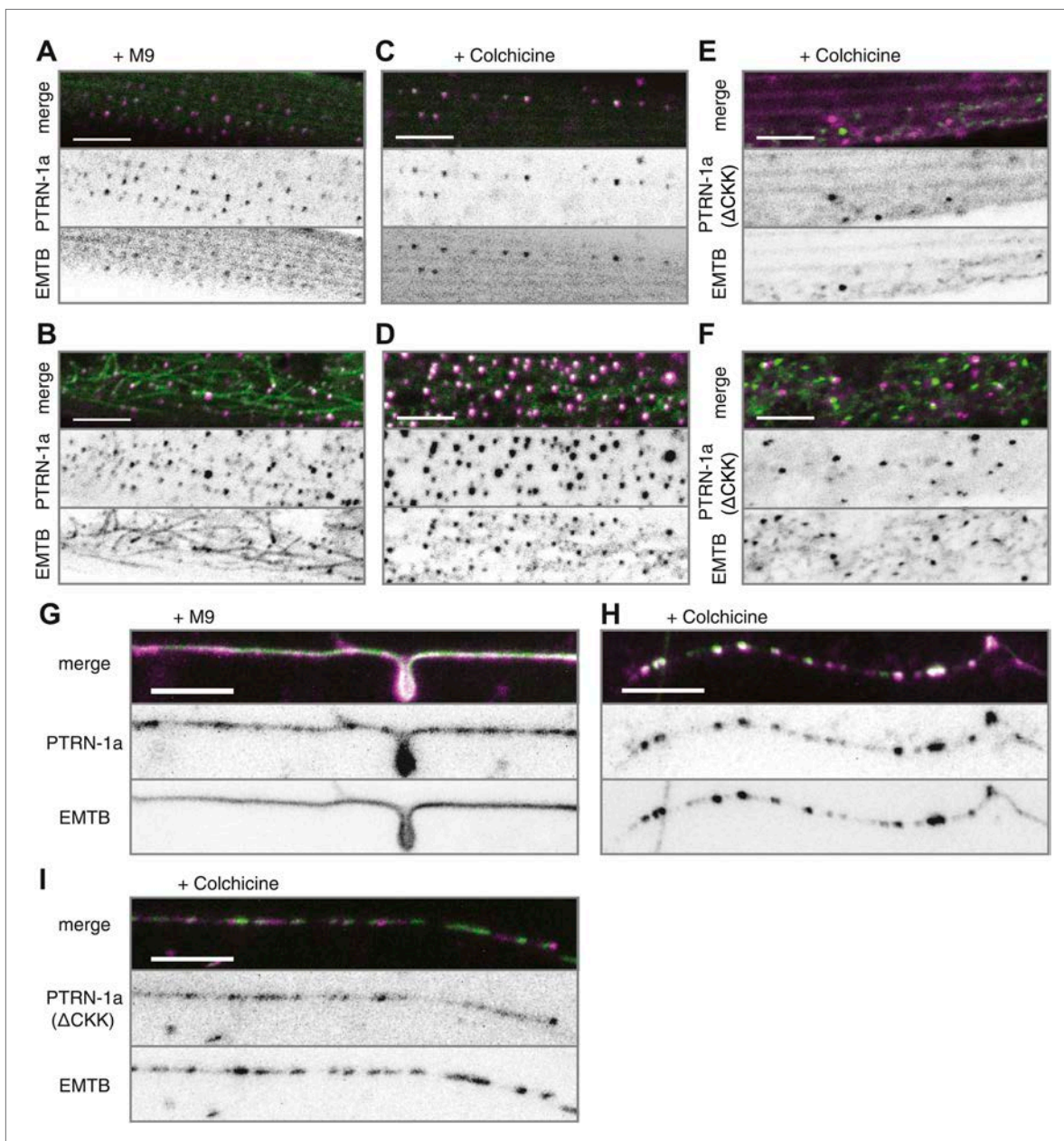


Figure 2. PTRN-1 stabilizes MT foci in neurons and muscles. (A–D) PTRN-1a::tdTomato and EMTB::GFP at the sarcolemma (A and C) and cell interior (B and D) of body wall muscle cells after acute colchicine exposure (C and D) or M9 control (A and B). (E and F) PTRN-1a(ΔCKK)::tdTomato and EMTB::GFP at the sarcolemma (E) and cell interior (F) of body wall muscle cells after acute colchicine exposure. (G–H) Localization of PTRN-1a::tdTomato and EMTB::GFP in the PVD dendrite after acute colchicine exposure (H) or M9 control (G). (I) PTRN-1a(ΔCKK)::tdTomato and EMTB::GFP in the PVD primary dendrite after acute colchicine exposure. All data acquired from *wyEx5968* with either *wyEx6022* (A–D and G and H), *wyEx6092* (I), or *wyEx6165* (E and F) co-expressed in *bus-17(e2800)* mutant animals. Scale bar: 5 μ m.

DOI: [10.7554/eLife.01498.009](https://doi.org/10.7554/eLife.01498.009)

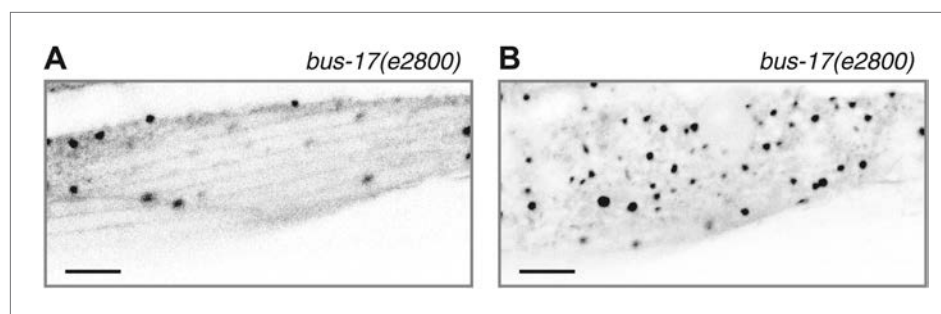


Figure 2—figure supplement 1. Acute colchicine exposure changes EMTB::GFP localization in body wall muscles.
DOI: [10.7554/eLife.01498.010](https://doi.org/10.7554/eLife.01498.010)

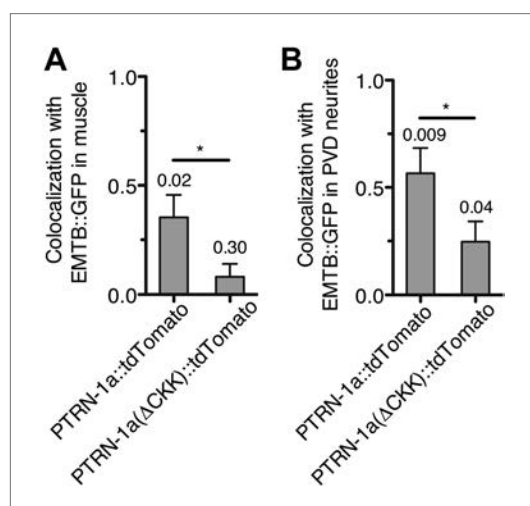


Figure 2—figure supplement 2. PTRN-1::tdTomato colocalizes with EMTB::GFP puncta after MT depolymerization by colchicine.
DOI: [10.7554/eLife.01498.011](https://doi.org/10.7554/eLife.01498.011)

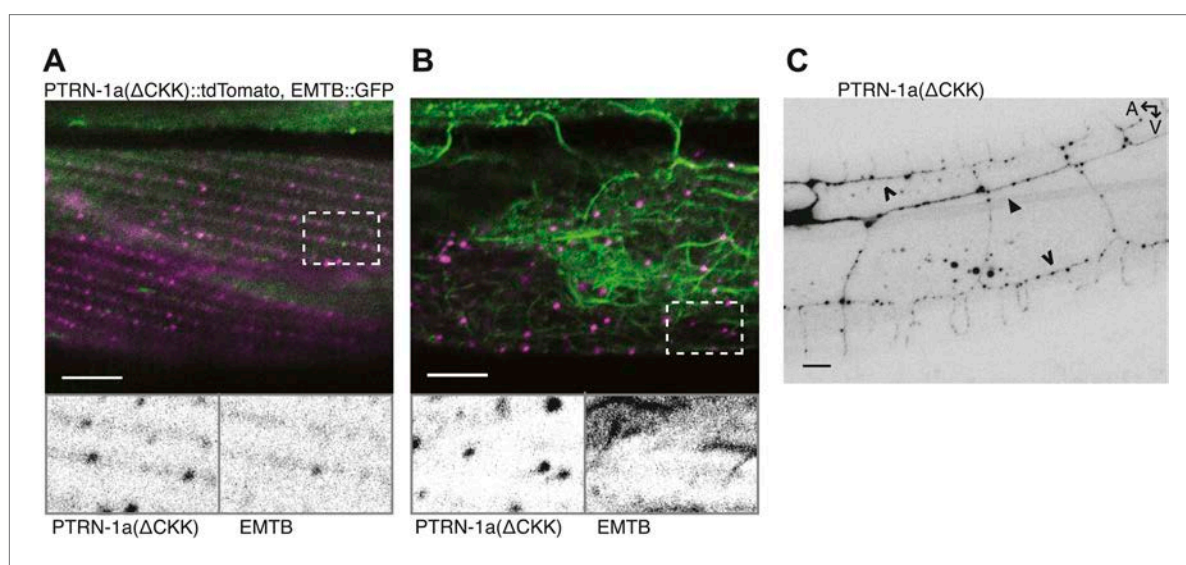


Figure 2—figure supplement 3. PTRN-1a(Δ CKK) exhibits punctate localization in body wall muscle cells and neurons.
DOI: [10.7554/eLife.01498.012](https://doi.org/10.7554/eLife.01498.012)

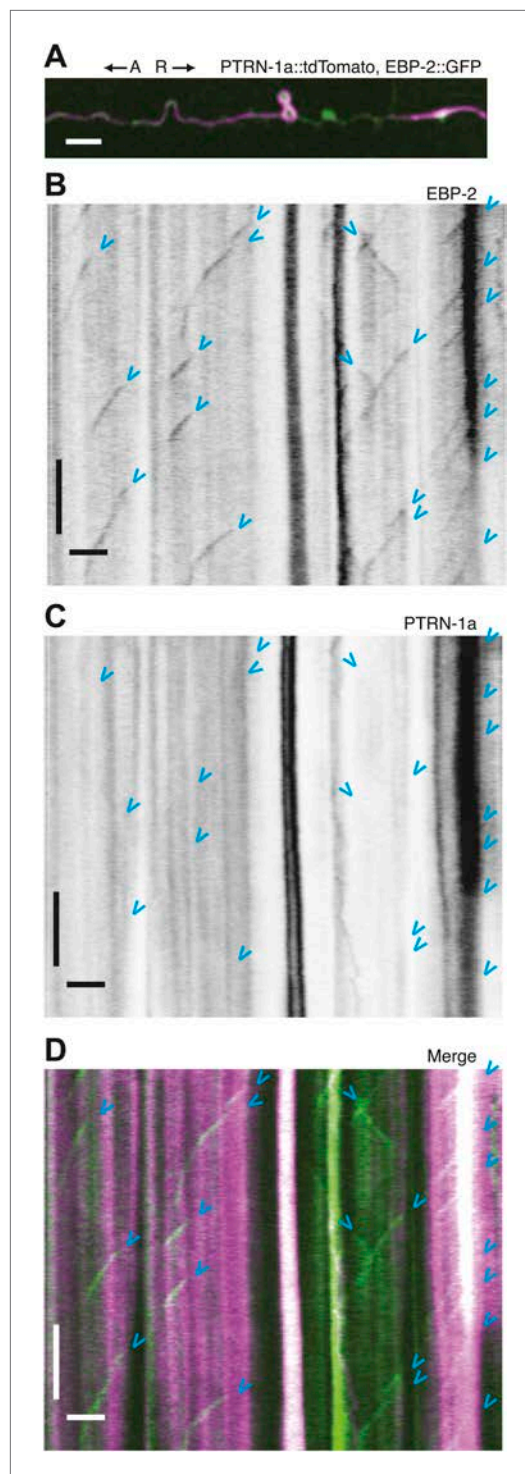


Figure 3. Immobility of PTRN-1a::tdTomato puncta contrasts with EBP-2::GFP movements in the PVD dendrite. **(A)** Live imaging was performed on a *ptrn-1(tm5597)* mutant animal co-expressing EBP-2::GFP (green, from the *wyEx4828* transgene), which labels growing plus-end of MTs, and PTRN-1a::tdTomato (magenta, from the *wyEx6022* transgene) along a section of the tertiary dendrite of the PVD neuron. **(B–D)**. Kymographs of EBP-2::GFP **(B)**, PTRN-1a::tdTomato **(C)**, and Merge **(D)**. Figure 3. Continued on next page

Figure 3. Continued

PTRN-1a::tdTomato (**C**), and overlay of EBP-2::GFP (green) with PTRN-1a::dtTomato (magenta) (**D**) from a 110 s video acquired from the PVD process shown in **A**. Time runs top to bottom. Arrows point to start of EBP-2::GFP movements. A, anterograde; R, retrograde. Scale bar: 5 μ m, ~22 s.

DOI: [10.7554/eLife.01498.013](https://doi.org/10.7554/eLife.01498.013)

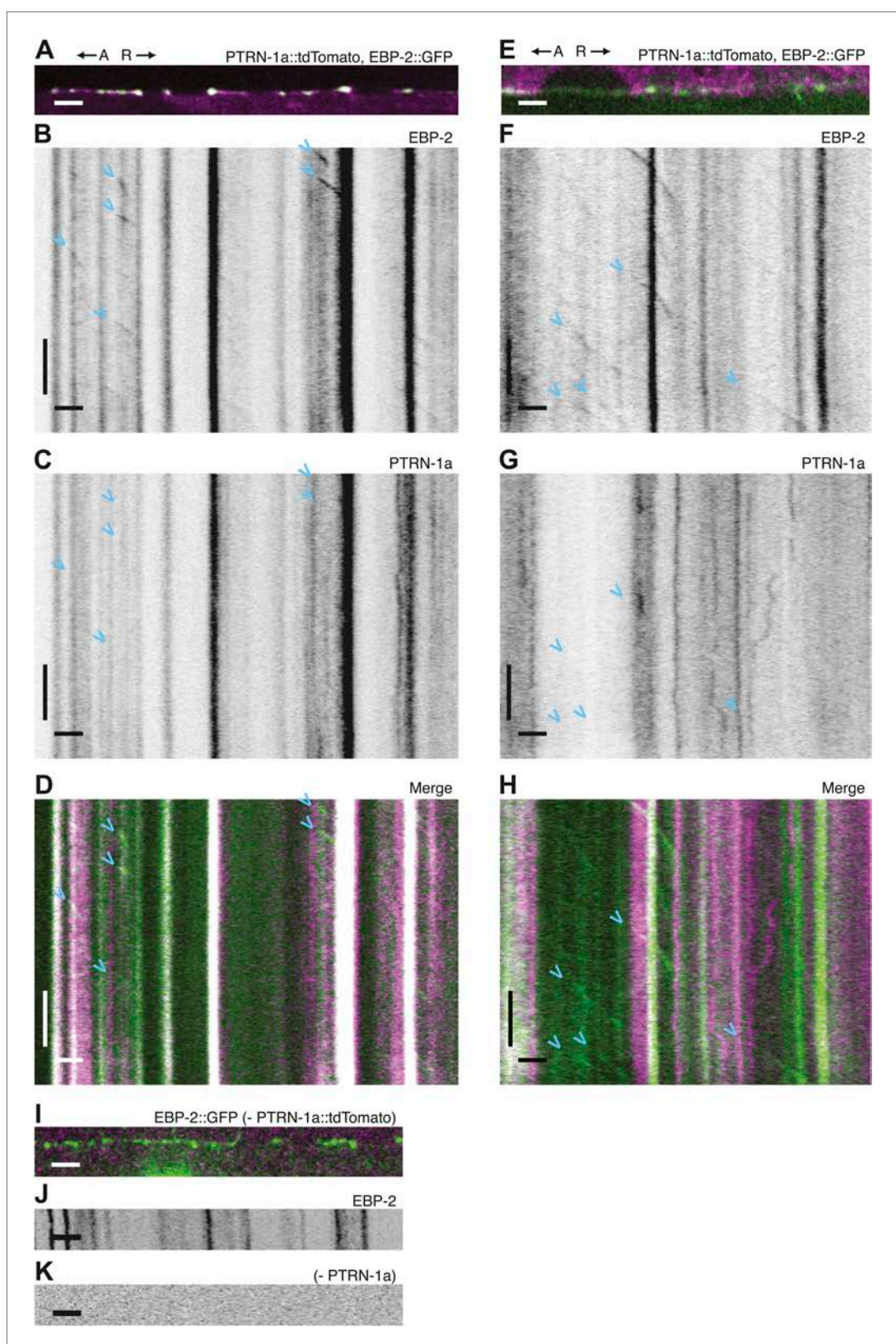


Figure 3—figure supplement 1. Immobility of PTRN-1a::tdTomato puncta contrasts with EBP-2::GFP movements in the PVD dendrite.

DOI: [10.7554/eLife.01498.014](https://doi.org/10.7554/eLife.01498.014)

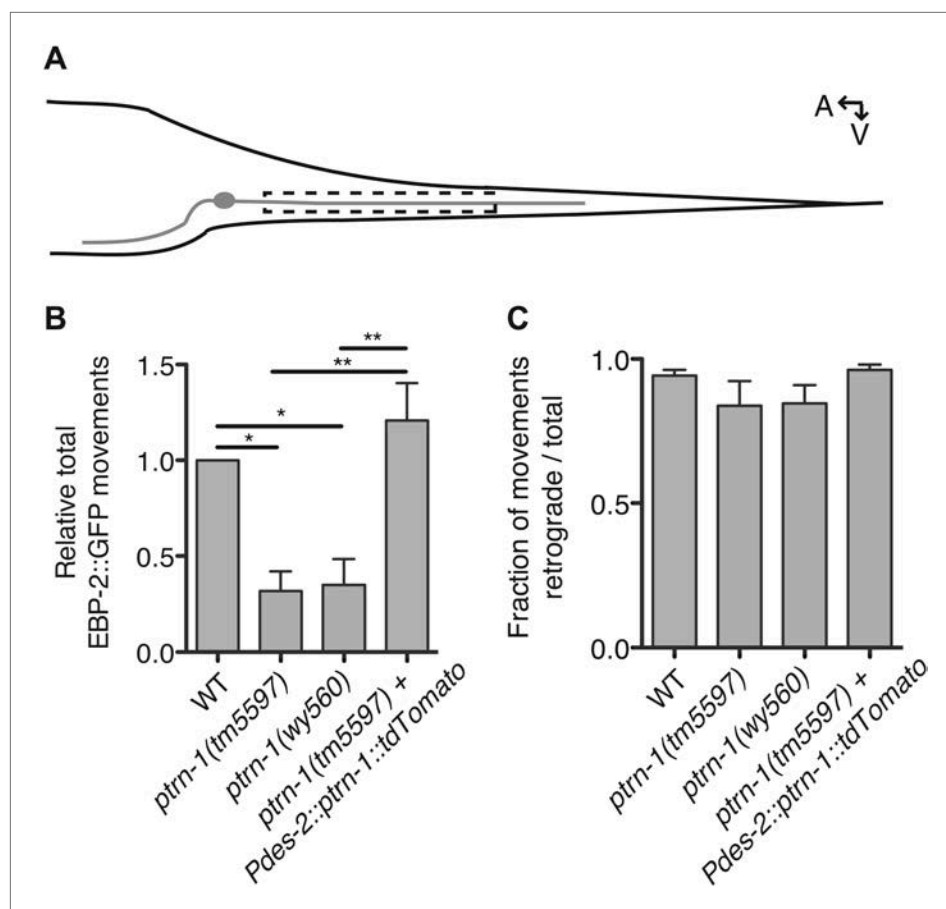


Figure 4. PTRN-1 promotes MT polymerization in neurites. **(A)** Schematic diagram of the PHC neuron. The anterior process is the axon; the posterior process is the dendrite. Live imaging was used to monitor EBP-2::GFP movements in the boxed region of the PHC dendrite. A: anterior, V: ventral. **(B and C)** Quantification of EBP-2::GFP anterograde and retrograde movements in the PHC dendrite of wild-type (WT) vs *ptrn-1(tm5597)* and *ptrn-1(wy560)* mutant animals, and vs the *ptrn-1(tm5597)* mutant carrying the *Pdes-2::ptrn-1::tdTomato* transgene, which is expressed in a subset of neurons as well as the body wall muscle. **(B)** Total EBP-2::GFP movements in each strain normalized against the wild-type control. **(C)** Fraction of EBP-2::GFP movements in each strain that moved in the retrograde direction. Mean \pm SEM. (n = 3 experiments, each with at least 10 animals/genotype, *p < 0.05, **p < 0.01, ANOVA with Bonferroni post test).

DOI: [10.7554/eLife.01498.017](https://doi.org/10.7554/eLife.01498.017)

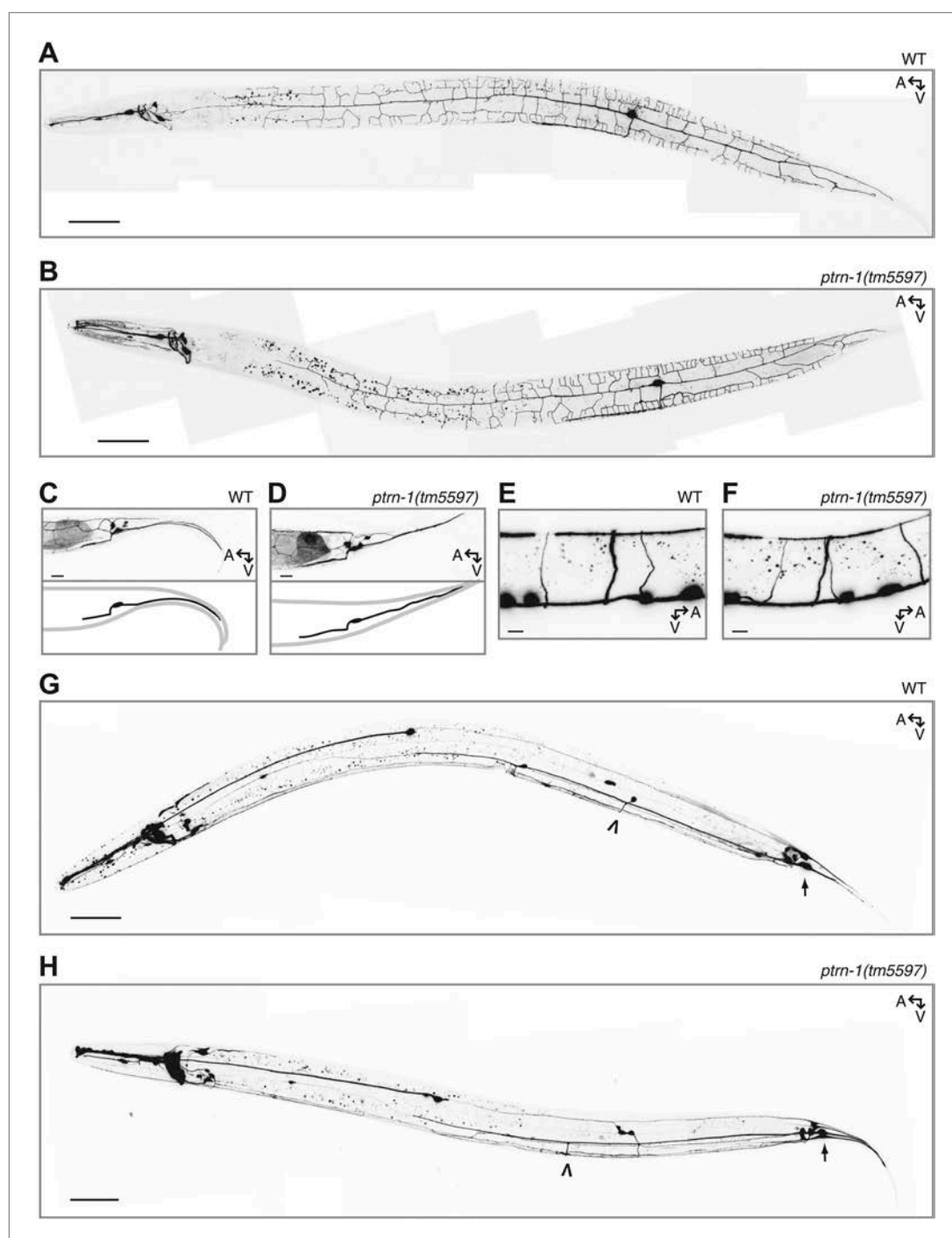


Figure 4—figure supplement 1. Neuronal morphology is grossly unaffected by loss of *ptrn-1*.

DOI: [10.7554/eLife.01498.018](https://doi.org/10.7554/eLife.01498.018)

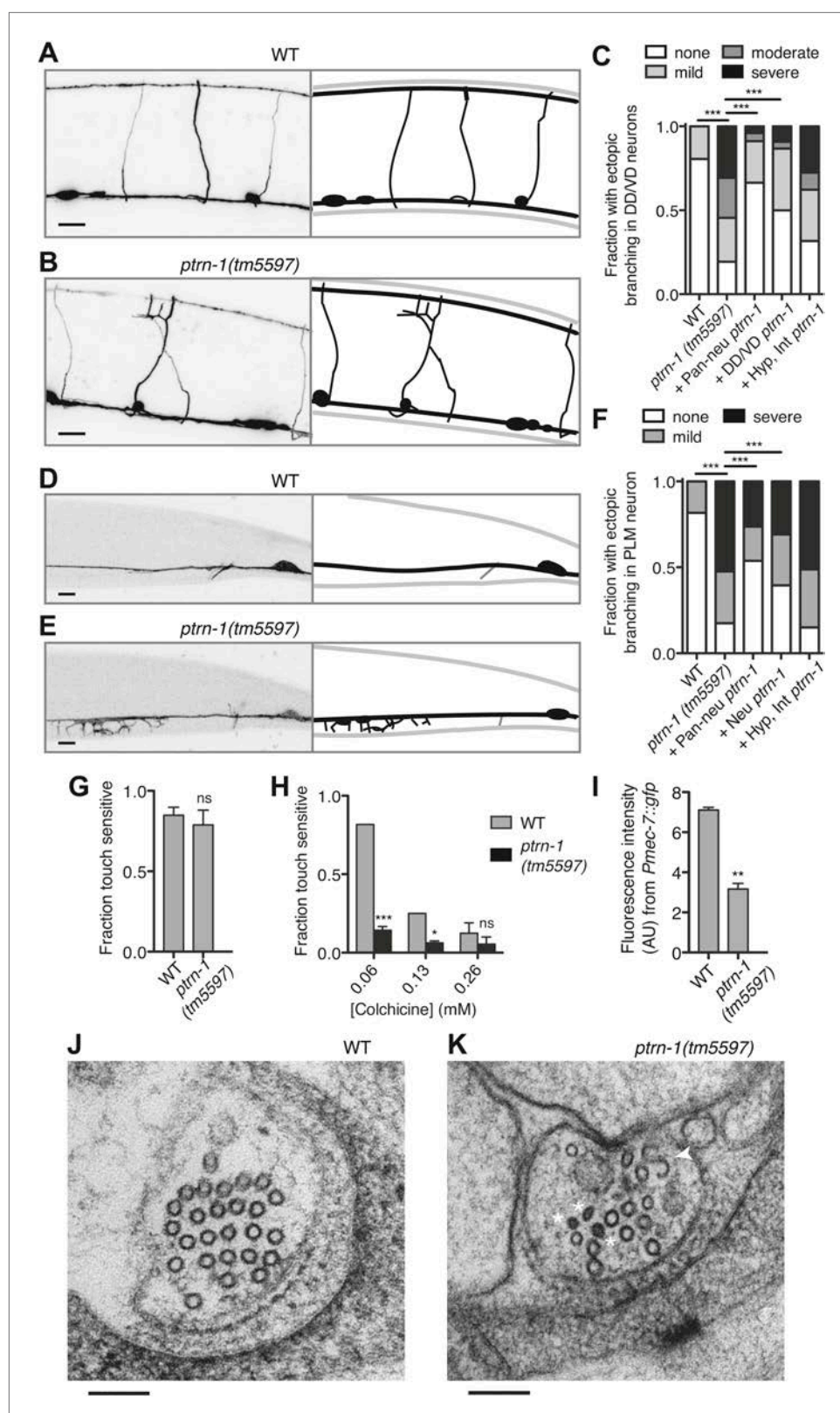


Figure 5. PTRN-1 supports MT stability in neurites. (A–C) Wild-type (A) and *ptrn-1(tm5597)* mutant (B) animals were grown in 0.13 mM colchicine to the L4 stage, and cytosolic RFP was used to visualize the DD/VD neurons. Scale bar: 10 μ m. (C) Fraction of animals with ectopic sprouting from the DD/VD neurons, scored based on severity as Figure 5. Continued on next page

Figure 5. Continued

described in 'Materials and methods' (n = at least 80 animals/genotype, ***p<0.001, Chi-squared test with Šidák correction). (D–F) Wild-type (D) and *ptrn-1(tm5597)* mutant (E) animals were grown in 0.035 mM colchicine to the L4 stage, and the PLM neuron was visualized with *myr::GFP*. Scale bar: 5 μ m. (F) Fraction of animals exhibiting ectopic sprouting from the PLM neuron, scored based on severity (n = at least 60 animals/genotype, ***p<0.001, Chi-squared test with Šidák correction). In schematic diagrams, the light gray lines represent the outline of the animal, DD and PLM neurons are black, and other neurons (in D and E only, one short, unbranched process near the PLM cell body of each image) are dark gray. For tissue specific rescue, DD/VD (*Punc-47L*), Pan-neu: pan-neuronal (*Prab-3*), Hyp: hypodermal (*Pdpy-7*), Int: intestinal (*Pvha-6*), neu: a subset of neurons including PLM (*Punc-86*). (G) Touch sensitivity of wild-type vs *ptrn-1(tm5597)* mutant animals. Mean \pm SEM. (n = 3 experiments, each with 8–12 animals/genotype, ns not significant (p=0.46), t test). (H) Touch sensitivity of wild-type vs *ptrn-1(tm5597)* mutant animals grown in the indicated concentrations of colchicine. Mean \pm SEM. (n = 2 experiments, each with 10 animals/genotype, ***p<0.001, *p<0.05, t test for each drug concentration). (I) Average fluorescence of GFP expressed from the *Pmec-7* (β -tubulin) promoter in the PLM cell body of wild-type vs *ptrn-1* mutant animals. Mean \pm SEM. (n = 2 experiments, each with at least 13 animals/genotype, **p<0.01, t test). (J and K) Transmission electron microscopy of the PLM neuron in wild-type (J) and *ptrn-1(tm5597)* mutant (K) young adult animals, sectioned near the rectum. Note MTs with abnormally smaller diameters (Asterisks), and a MT sheet shaped like an 'S' (Arrow head). Scale bar: 100 nm.

DOI: [10.7554/eLife.01498.019](https://doi.org/10.7554/eLife.01498.019)

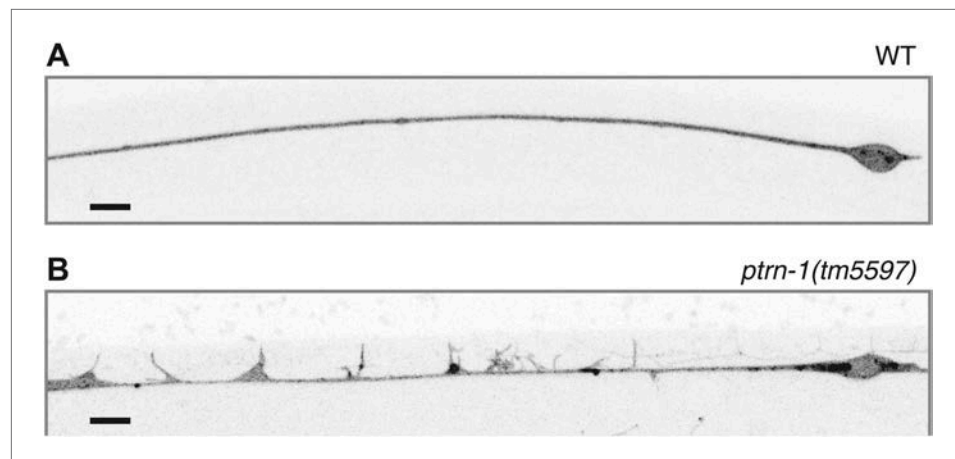


Figure 5—figure supplement 1. PTRN-1 protects the ALM touch receptor neuron against ectopic neurite sprouting during growth in colchicine.

DOI: [10.7554/eLife.01498.020](https://doi.org/10.7554/eLife.01498.020)

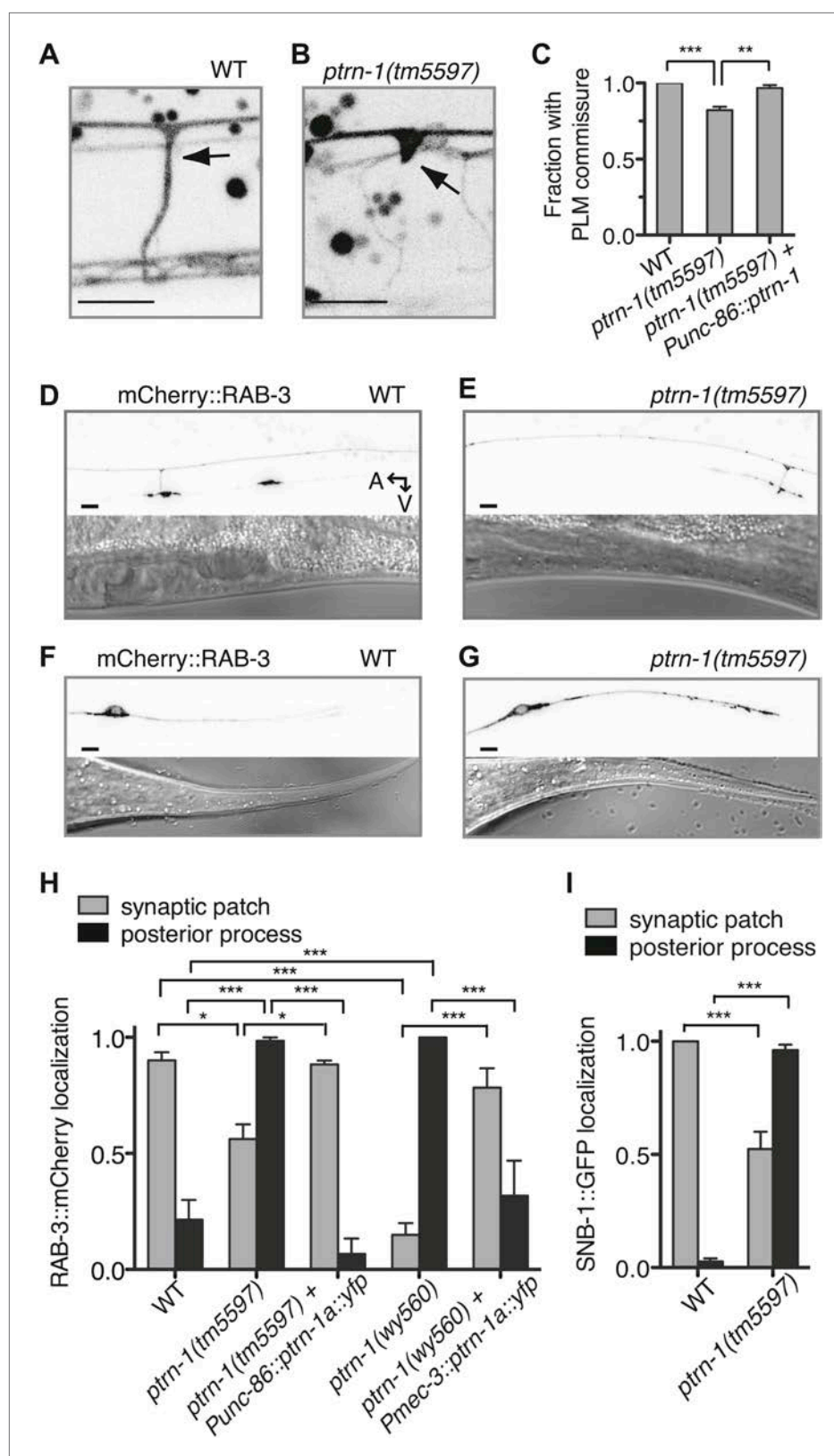


Figure 6. PTRN-1 promotes synapse localization and neurite morphology in the PLM neuron. (A and B) myrGFP was used to visualize the PLM commissure in wild-type (A) and *ptrn-1(tm5597)* mutant (B) animals. Arrows point to commissure or commissure bud. (C) Fraction of animals with a PLM commissure connecting the axon to the ventral Figure 6. Continued on next page

Figure 6. Continued

nerve cord. Mean \pm SEM. (n = 3 experiments, each with at least 30 animals/genotype, **p<0.01, ***p<0.001, one-way ANOVA with Bonferroni post test). (D and E) mCherry::RAB-3 at the synaptic patch of the PLM neurons of wild-type (D) and *ptrn-1(tm5597)* mutant (E) animals. (F and G) mCherry::RAB-3 in the posterior process of the PLM neurons in wild-type (F) and *ptrn-1(tm5597)* mutant (G) animals. (H) Fraction of wild-type and *ptrn-1* mutant animals with visible accumulation of mCherry:RAB-3 at the synaptic patch and the posterior process of the PLM neuron. The *Punc-86* promoter is expressed in a subset of neurons including the TRNs; the *Pmec-3* promoter is expressed in the TRNs. Animals with two visible mCherry:RAB-3 patches in the PLM synaptic region were counted as having synaptic accumulation, and animals with one or no visible mCherry::RAB-3 patches were considered to have loss of synaptic accumulation. Mean \pm SEM. (n = 2 experiments, each with 30 animals/genotype, *p<0.05, ***p<0.001, two-way ANOVA with Bonferroni post test). (I) Fraction of wild-type and *ptrn-1(tm5597)* mutant animals with visible accumulation of SNB-1::GFP at the synaptic patch and the posterior process of the PLM neuron. Synaptic patch accumulation was scored as in H. Mean \pm SEM. (n = 2 experiments, each with at least 20 animals/trial. ***p<0.001, two-way ANOVA with Bonferroni post test).

DOI: [10.7554/eLife.01498.021](https://doi.org/10.7554/eLife.01498.021)

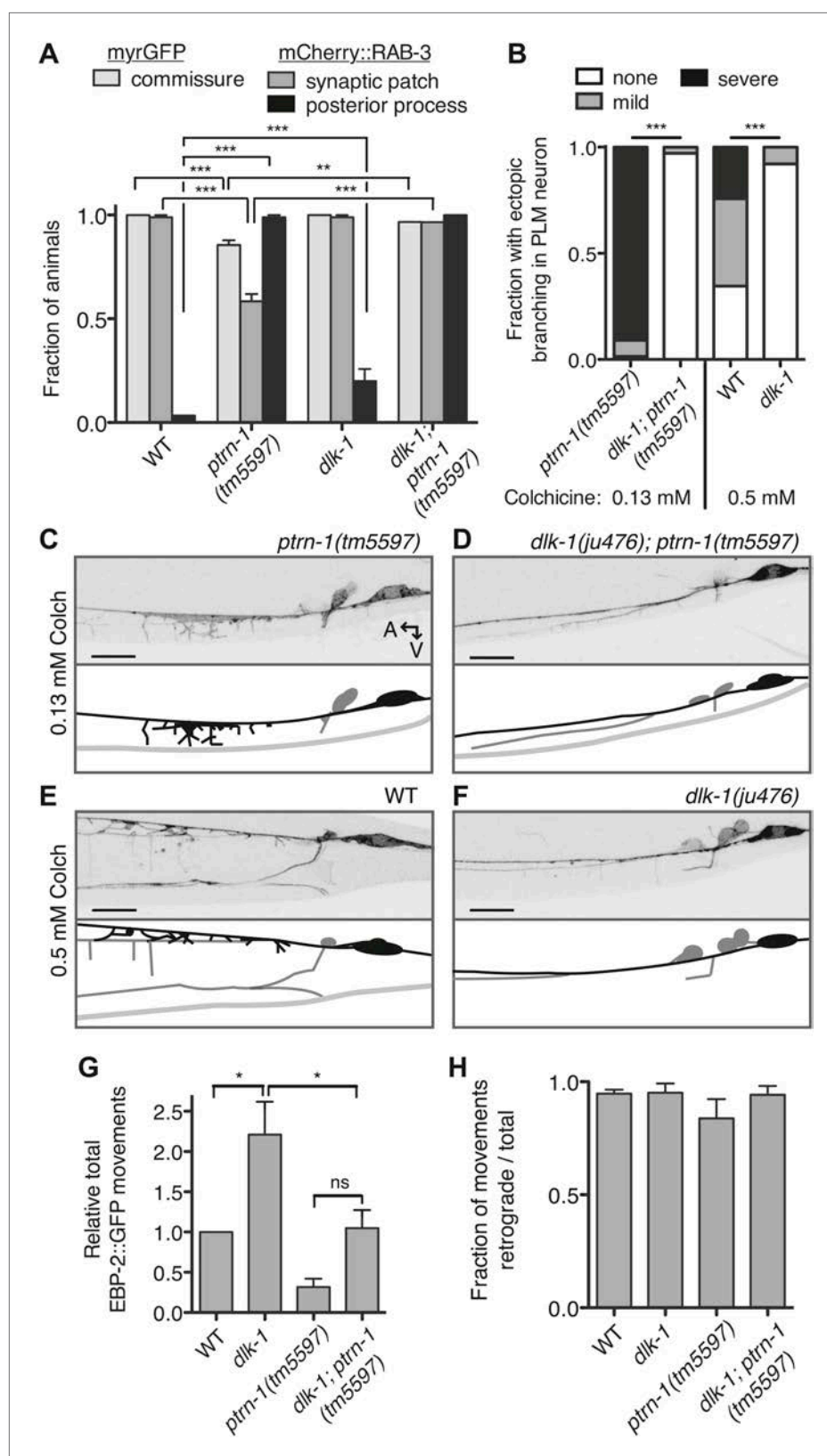


Figure 7. Aberrant phenotype of the PLM neuron in the *ptrn-1* mutant is mediated partially by the DLK-1 pathway. (A) The *wyls97*(*Punc-86::myrGFP*, *Punc-86::mCherry::rab-3*) transgene was used to simultaneously visualize commissure formation and SV localization. Only animals with an intact PLM commissure were counted for Figure 7. Continued on next page

Figure 7. Continued

mCherry::RAB-3 localization at the synaptic patch. Values represent mean \pm SEM. (n = 3 experiments, each with at least 30 animals/genotype, **p<0.01, ***p<0.001, two-way ANOVA with Bonferroni post test). (B–F) Animals were grown in 0.13 mM colchicine (C and D) or 0.5 mM colchicine (E and F) to the L4 stage, and the PLM neuron was visualized with myr::GFP. In schematic diagrams, the PLM neurons are black, and other neurons in the image are dark gray. (B) Fraction of animals exhibiting ectopic sprouting from the PLM neuron, scored based on severity (n = at least 120 animals/genotype, ***p<0.001, Chi-squared test for each drug concentration). (G and H) Quantification of EBP-2::GFP anterograde and retrograde movements in the PHC dendrite. (G) Total EBP-2::GFP movements in each strain normalized against the wild-type control. (H) Fraction of EBP-2::GFP movements in each strain that moved in the retrograde direction. Mean \pm SEM. (n = 3 experiments, each with at least 9 animals/genotype, *p<0.05, ns not significant, one-way ANOVA with Bonferroni post test. The data for the *ptrn-1* single mutant is the same as that shown in Figure 4).

DOI: [10.7554/eLife.01498.022](https://doi.org/10.7554/eLife.01498.022)

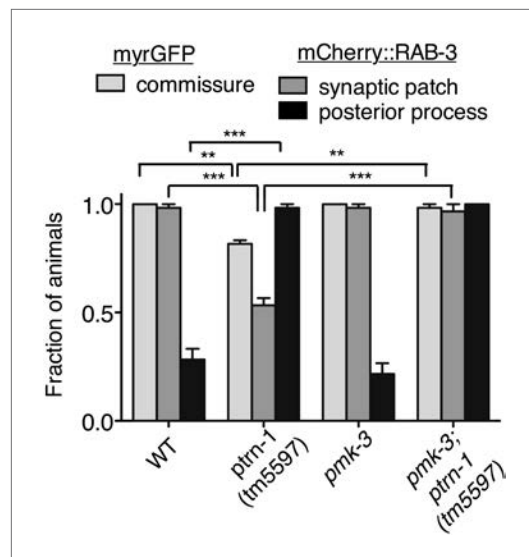


Figure 7—figure supplement 1. Loss of *pmk-3* partially suppresses the aberrant phenotype of the PLM neuron in the *ptrn-1* mutant.

DOI: [10.7554/eLife.01498.023](https://doi.org/10.7554/eLife.01498.023)